

Electron–positron pair production and annihilation spectral features from compact sources

Andrzej Maciołek-Niedźwiecki,¹ Andrzej A. Zdziarski¹ and Paolo S. Coppi²

¹*N. Copernicus Astronomical Center, Bartycka 18, 00-716 Warsaw, Poland, Internet: (aaz, amaniem)@camk.edu.pl*

²*Department of Astronomy, Yale University, Box 208101, New Haven, CT 06520, USA*

Accepted 1995 March 30. Received 1995 February 6

ABSTRACT

We study the efficiency of e^\pm pair production in compact γ -ray sources, as measured by the fraction of power supplied to a source that is converted into pair annihilation radiation emitted by the source (the pair yield). We focus mainly on thermal plasmas, in contrast to previous studies of the pair yield in nonthermal plasmas. We calculate the pair yield in thermal plasmas where bremsstrahlung is the only source of soft photons as well in plasmas in which there is a copious source of soft photons. We find that the pair yield reaches its maximum of ~ 0.3 in Comptonized bremsstrahlung plasmas. The corresponding maximum fraction of source power converted into pair rest mass is ~ 0.2 . Addition of ambient soft photons to the source reduces the pair yield. The maximum yield is still close to ~ 0.3 in plasmas where the soft photons are Comptonized into hard power laws of energy spectral index $\alpha \simeq 0.1$ – 0.2 , but decreases with increasing α and becomes < 0.01 for $\alpha \gtrsim 0.7$. Even when the pair yield is large, we never find an observable annihilation feature from a thermal plasma. To have a high pair yield, typically either the plasma temperature must be relativistic or photons must undergo many Compton scatterings before escaping the source. Hence, the emergent annihilation spectrum is either intrinsically broad or strongly smeared by repeated Compton scatterings and is difficult to distinguish from the underlying Compton scattering and bremsstrahlung continuum. This is in contrast to the nonthermal case where strong, narrow annihilation features can be produced by pairs which have cooled in the source. We summarize the conditions when such strong features are produced, and calculate the pair yield when primary electrons are injected with power-law energy distributions.

While observable annihilation features are not produced directly in thermal sources, strong pair outflows, e.g., electron–positron jets, may be created in sources with hard spectra. The outflowing pairs may cool and annihilate *outside* the source region, in which case a visible annihilation feature is possible. However, our results applied to Nova Muscae show that neither thermal nor nonthermal pair models can explain the large strength of the annihilation feature observed from that source (unless a complex obscuration scenario is invoked). On the other hand, the annihilation feature of the 1979 March 5 γ -ray burst can be explained by our models provided the source is located at a distance much less than that to the LMC.

Key words: plasmas – radiation mechanisms: nonthermal – stars: individual: Nova Muscae – gamma-rays: theory.

1 INTRODUCTION

The question of the presence of e^\pm pairs in compact X-ray and γ -ray sources remains a major unresolved astrophysical problem. Recent observations of Seyfert-type AGNs by the OSSE detector aboard *GRO* indicate that their X-ray and soft γ -ray emission is either from thermal plasmas or from non-thermal ones where most of the nonthermal power goes into low-energy particles (Maisack et al. 1993; Zdziarski, Lightman

& Maciołek-Niedźwiecki 1993; Zdziarski et al. 1994, 1995; Madejski et al. 1995). However, these data do not yet allow us to determine whether the plasmas consist of e^\pm pairs or of electrons and protons. In particular, the upper limits on the strength of possible annihilation features around 511 keV are only weakly constraining. The important question of whether e^\pm pairs are present in the parsec-scale jets of radio-loud AGNs remains similarly unresolved (Ghisellini et al. 1992). On the other hand, strong transient features at ~ 511 keV

have been discovered in the spectra of some Galactic sources by the SIGMA detector aboard *GRANAT* (Gilfanov et al. 1994) and by *HEAO-1 A4* (Briggs et al. 1995). It is tempting to infer that these features are produced by the annihilation of large numbers of pairs in the plasma responsible for the source continuum emission. However, relatively complex models invoking additional ingredients such as the obscuration of the continuum emission region appear to be required to make such an interpretation tenable (e.g., Maciołek-Niedźwiecki & Zdziarski 1994).

Motivated by these observational developments and interest in what constraints arise from the detection or non-detection of a pair annihilation feature, we study here the efficiency of production of e^\pm pairs in compact plasmas. This efficiency determines the overall intensity of the plasma's pair annihilation emission and is conveniently described by the pair yield, which we define as the fraction of the power supplied to a source converted into the energy of pair-annihilation photons that escape the source. The knowledge of the pair yield is also necessary to make predictions of the abundance of pairs in astrophysical sources as well as predictions of the flux of outflowing pairs that might form winds and jets in these sources (Ghisellini et al. 1992). The pair yield has already been studied before for some nonthermal plasmas (Svensson 1987; Lightman & Zdziarski 1987; Zdziarski, Coppi & Lamb 1990; Done, Ghisellini & Fabian 1990). Consequently, our study focuses mainly on the pair yield produced in thermal plasmas. In addition, we study nonthermal plasmas in which electrons are injected with a spread of energies. Recent OSSE observations imply that plasmas of either kind might exist in Seyfert AGNs (e.g., Maisack et al. 1993; Zdziarski et al. 1994). In addition, we study the spectra produced by thermal plasmas with pairs in order to determine if annihilation features are observable when the pair yield is large.

In Section 2, we calculate the pair yield and the spectra for thermal plasmas where bremsstrahlung is the only source of soft photons, as well as in plasmas with copious ambient soft photons. In Section 3, we study the pair yield in plasmas with nonthermal power-law electron injection. In Section 4, we discuss applications of our results to Galactic sources emitting ~ 500 -keV spectral features, to AGNs, and to the 1979 March 5 γ -ray burst.

2 THERMAL PLASMAS

We study here the efficiency of e^\pm pair production in thermal plasmas in pair equilibrium. We assume a spherical source geometry, with a characteristic source size R . In some cases we take into account escape of pairs from the source (Zdziarski 1985, hereafter Z85) by introducing the dimensionless parameter

$$\beta = \frac{R/c}{n_+ / (\dot{n}_+)_{\text{esc}}}, \quad (1)$$

where $(\dot{n}_+)_{\text{esc}}$ is the pair escape rate averaged over the source volume, and n_+ is the positron density.

At relativistic temperatures, some part of the power supplied to the source is used for the production of e^\pm pairs in photon–photon, photon–electron and electron–electron interactions. The proton processes ($pe \rightarrow pee^+e^-$ and $p\gamma \rightarrow pe^+e^-$) are at least an order of magnitude slower than the correspond-

ing electron processes (Zdziarski 1982; those processes also do not take place in a pure pair plasma) and they are neglected in this paper. We use equation (B1) in Svensson (1984, hereafter S84) for the photon–photon pair production rate and equation (13) from Z85 for the photon–electron pair production rate. For the pair production rate by electron–electron collisions, we use equation (14) from Z85. We neglect pair production by annihilation photons as it has a small effect on pair equilibrium.

The processes of pair production and thermalization convert a fraction of the total source power into both pair rest mass and pair kinetic energy. We define ℓ_{esc} as the compactness parameter [$\ell \equiv L\sigma_T/(m_e c^3 R)$, where L is a luminosity] corresponding to the power going into the rest + kinetic energy of pairs escaping the source:

$$\ell_{\text{esc}} = \beta u \frac{4\pi}{3} \tau \left[3\Theta + \frac{K_1(1/\Theta)}{K_2(1/\Theta)} \right], \quad (2)$$

where $\Theta \equiv kT/(m_e c^2)$, the expression in brackets is the average energy of a particle (equal to $3\Theta/2 + 1$ when $\Theta \ll 1$ and 3Θ when $\Theta \gg 1$), $u \equiv 2n_+/n_e$ is the pair abundance, K_n is the modified Bessel function of the second kind of order n , and $\tau (= n_e \sigma_T R)$, where $n_e = n_+ + n_-$ is the sum of the positron and electron densities, and σ_T is the Thomson cross-section) is a Thomson optical depth. (Note that ℓ_{esc} can be larger than the compactness in annihilation outside the source: see below and Appendix.) Some of the pairs produced annihilate inside the source. We therefore define an additional compactness parameter corresponding to the source power that goes in annihilation photons that escape the source:

$$\ell_{\text{ann}} = \frac{\pi}{4} \frac{u(2-u) \min(\tau^2, 2.33\tau)}{1/(1+6\Theta) + \Theta/[\ln(1.12\Theta + 1) + 0.25]} \quad (3)$$

[cf. equation (16) in Svensson (1982)]. Note that our definition of ℓ_{ann} includes only those annihilation photons that escape from the source unscattered. Annihilation photons that scatter (with $\sigma \simeq 0.43\sigma_T$) lose most of their energy and can be neglected in the energy balance. Finally, we define a total pair compactness parameter, $\ell_{\text{pair}} = \ell_{\text{ann}} + \ell_{\text{esc}}$, which corresponds to the total power carried away from the source by escaping pairs and annihilation radiation.

In thermal, optically thick plasmas the pair yield can be defined in various ways, namely, including or neglecting the kinetic energy of annihilating pairs and including or neglecting the effect of scattering of annihilation photons. Our definition includes the kinetic energy and takes into account scattering:

$$Y = \frac{\ell_{\text{pair}}}{\ell_{\text{tot}}} \quad (4)$$

(where ℓ_{tot} is the total power supplied to the source), and gives the efficiency at which both annihilation photons and thermal pairs leave the source. This definition gives us the maximum fraction of source luminosity that can be transformed into observable annihilation radiation. (The energy of escaping pairs should be included since these pairs can annihilate outside the source.) In some cases, we will also consider the pair yield including only the rest mass of pairs, denoted by Y^0 .

We also define the fractional quantities corresponding to annihilation and pair escape,

$$Y_{\text{ann}} = \ell_{\text{ann}}/\ell_{\text{tot}}, \quad Y_{\text{esc}} = \ell_{\text{esc}}/\ell_{\text{tot}}. \quad (5)$$

Pairs annihilate inside the source at the electron temperature, Θ . However, escaping pairs may lose their kinetic energy before annihilation. Therefore, we will consider also the quantity

$$Y_{\text{esc}}^0 = \ell_{\text{esc}}^0 / \ell_{\text{tot}}, \quad (6)$$

where $\ell_{\text{esc}}^0 = 4\pi\beta u\tau/3$ is the compactness parameter corresponding to the power carried in the rest mass energy of escaping pairs. The actual fraction of the source luminosity due to annihilation of pairs outside the source will be between Y_{esc}^0 and Y_{esc} , depending on the efficiency of cooling mechanisms.

2.1 Comptonized bremsstrahlung

In this section we study plasmas where bremsstrahlung is the only source of soft photons. Following S84, we assume that the spectrum of Comptonized bremsstrahlung can be represented as a sum of a flat bremsstrahlung spectrum and a Wien spectrum [see equations (3.5)–(3.6) in S84]:

$$N(\epsilon) = N_{\text{brem}} \frac{e^{-\epsilon/\Theta}}{\epsilon} + \frac{1}{2} N_{\text{W}} \left(\frac{\epsilon}{\Theta} \right)^3 \frac{e^{-\epsilon/\Theta}}{\epsilon}, \quad (7)$$

where $\epsilon \equiv E/m_e c^2$, E is the photon energy,

$$N_{\text{brem}} = \frac{8\pi\Theta\epsilon_m^2}{\lambda^3} \left[\frac{1}{\ln(\Theta/\epsilon_m)} + \frac{y_1}{1+y_1} \right], \quad (8)$$

and

$$N_{\text{W}} = \frac{R}{c} \left[1 + \frac{1}{3} \tau_{\text{W}}(\Theta) \right] \dot{N}_{\text{brem}} f_{\text{W}}. \quad (9)$$

Here λ is the electron Compton wavelength, ϵ_m is the energy below which photons are self-absorbed, \dot{N}_{brem} is the total bremsstrahlung photon production rate above ϵ_m , $\tau_{\text{W}}(\Theta)$ is the scattering optical depth averaged over a Wien distribution [equation (B14) in S84] and f_{W} is the probability that a photon is scattered into the Wien peak before escaping:

$$f_{\text{W}} = 2 \left[y_1^2 - (y_1 + y_1^2) \exp(-1/y_1) \right], \quad (10)$$

with

$$y_1 = \frac{\tau^2 \ln(1 + 4\Theta + 16\Theta^2)}{3 \ln(\Theta/\epsilon_m)}. \quad (11)$$

A model is specified by Θ , the proton density n_p , and $\tau_p = n_p \sigma_{\text{T}} R$ (the proton optical depth). The pair abundance, u , is given by the solution of the pair equilibrium equation (pair production rate = pair annihilation rate) and the equation for ϵ_m [see equation (D4) in S84],

$$n_e \sigma_{\text{T}} = a_{\text{abs}}(\epsilon_m) \frac{\tau(1 + \tau/3)}{1 + \tau^2 \min(1, 8\Theta)/3}, \quad (12)$$

where a_{abs} is the bremsstrahlung absorption coefficient. For given τ_p and n_p , there are two solution branches, the low- u and high- u , that merge at a temperature $\Theta_c(\tau_p, n_p)$. Above Θ_c , there are no equilibrium solutions as pair production is faster than annihilation.

In energy equilibrium, the total power provided to the source equals the sum of bremsstrahlung, Comptonization into the Wien component, and annihilation cooling rates. Denoting the compactness parameters corresponding to these processes as ℓ_{brem} , ℓ_{W} and ℓ_{ann} , respectively, we can write the pair yield as

$$Y = \frac{\ell_{\text{ann}}}{\ell_{\text{brem}} + \ell_{\text{W}} + \ell_{\text{ann}}}, \quad (13)$$

where ℓ_{ann} is given by equation (3), ℓ_{brem} is

$$\ell_{\text{brem}} = \frac{\alpha_{\text{f}} \tau^2}{2} \left[(1-u) f_{\text{ep}}(\Theta) + (u^2 - 2u + 2) \frac{f_{\text{ee}}(\Theta)}{2} + u(2-u) \frac{f_{\pm}(\Theta)}{4} \right] \quad (14)$$

[α_{f} is the fine-structure constant, f_{ep} , f_{ee} and f_{\pm} are defined by the Θ -dependent terms of the bremsstrahlung cooling rates given by equations (17)–(22) in Svensson (1982)], and

$$\ell_{\text{W}} = 4\pi\Theta f_{\text{W}} \dot{N}_{\text{brem}} \frac{\sigma_{\text{T}}}{c} R^2 \propto \tau^2 \quad (15)$$

[from equation (17) in Björnsson & Svensson (1991)].

Fig. 1(a) shows the values of Y in models with $n_p = 10^{11} \text{ cm}^{-3}$ (the dependence of the solution on n_p is weak). There is negligible pair production on the low- u branch. On the high- u branch and at a given Θ , Y increases with decreasing τ_p . For a given τ_p , Y achieves the highest values of $Y \gtrsim 0.2$ for $\Theta \simeq 0.2$ – 0.8 . The maximum pair yield of $Y = 0.28$ is achieved for $\Theta = 0.4$ and $\tau_p < 0.5$. The corresponding $Y^0 = 0.18$.

For $\Theta \lesssim 0.3$, the plasma is optically thick and Wien equilibrium is approached (S84). The pair yield in Wien equilibrium was considered by Kusunose & Zdziarski (1994). They found that the power converted into pair rest mass inside the source may exceed the radiative luminosity. However, although pairs may be created at such a rate, the rate of escape of annihilation photons is much less due to scattering. This effect is included in our definition of Y , which is always < 1 . The decline of Y with decreasing Θ at $\Theta \lesssim 0.3$ (for which the pair production rate inside the source keeps increasing) seen in Fig. 1(a) is due to downscattering of annihilation photons when the plasma becomes optically thick. At $\Theta \ll 1$, the emitted annihilation feature is weak and completely masked by the strong Wien spectrum (see Zdziarski 1984). At $\Theta \gtrsim 0.3$, the relative amplitude of the Wien spectrum declines, but this effect is compensated by the annihilation spectrum becoming broader, with its width proportional to the pair temperature. For no plasma parameters is there an observable annihilation feature.

Fig. 1(b) shows the pair yield as a function of the total compactness, $\ell_{\text{tot}} \equiv \ell_{\text{brem}} + \ell_{\text{W}} + \ell_{\text{ann}}$, rather than the temperature. We see that the Y has rather sharp maxima at $\ell_{\text{tot}} \simeq 20$ – 25 .

2.2 Comptonization of soft photons

In this section we consider plasmas that emit power-law spectra produced by the repeated Compton scattering of some copious source of soft photons by relativistic thermal electrons. (For example, the soft photons could be UV or soft X-rays from an optically thick accretion disc, or self-absorbed cyclotron emission. Such photons are hereafter referred to as ‘ambient’ soft photons.) The total spectrum can be represented as

$$N(\epsilon) = \left[N_{\text{brem}} + \frac{1}{2} N_{\text{P}} \left(\frac{\epsilon}{\Theta} \right)^{-\alpha} + \frac{1}{2} N_{\text{W}} \left(\frac{\epsilon}{\Theta} \right)^3 \right] \frac{e^{-\epsilon/\Theta}}{\epsilon}, \quad (16)$$

where N_{W} is due to Comptonization of both bremsstrahlung (equation 15) and ambient photons (Z85). For strong enough soft-photon input, N_{brem} can be neglected in comparison with N_{P} (see below).

For a plasma with given Θ and τ , α is determined by equations (2)–(7) in Z85. Here, we invert this relation and use

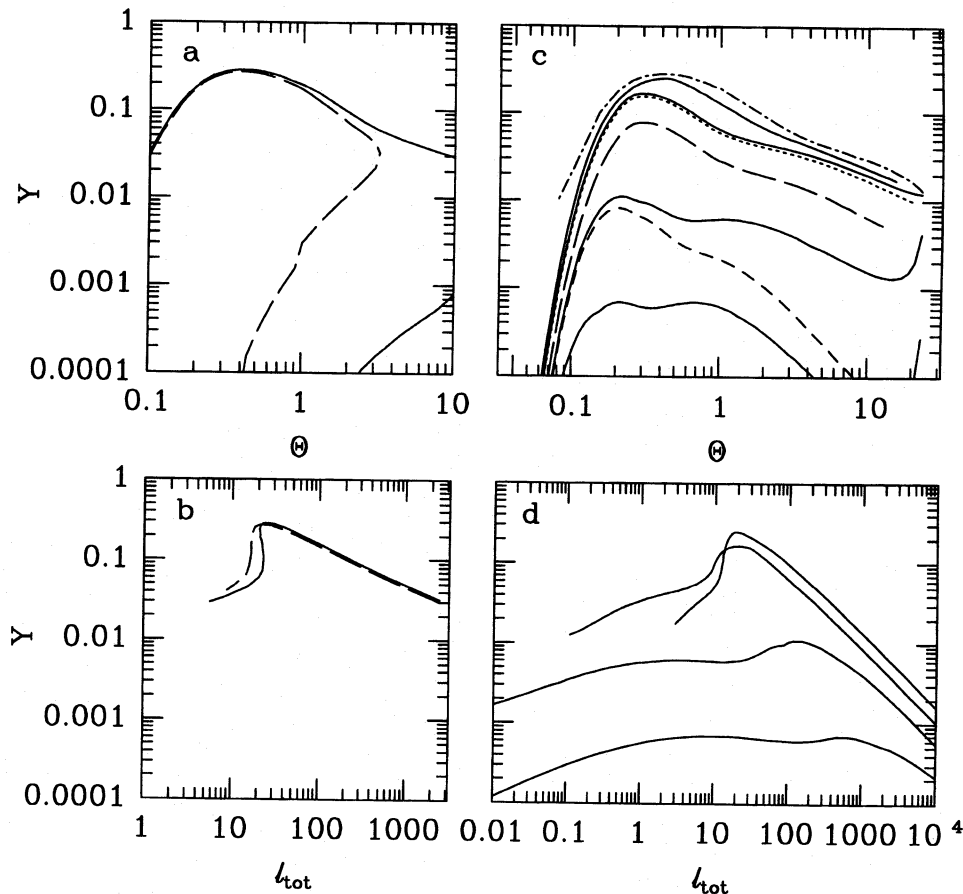


Figure 1. The pair yield in plasmas with no pair escape. Comptonized bremsstrahlung: (a) The solid and dashed curves give Y as functions of Θ for $\tau_p = 0.1$ and 1 , respectively. The overall maximum pair yield in thermal plasmas, $Y = 0.28$, is achieved for $\tau_p < 0.5$ and $\Theta \simeq 0.4$. (b) The dependence of Y on ℓ_{tot} . The meaning of curves is the same as in (a). Note the sharp maxima at $\ell_{\text{tot}} \sim 20$. Comptonization of ambient soft photons: (c) $Y(\Theta)$. From top to bottom, the solid curves give Y for $u = 1$, and $\alpha = 0.14, 0.3, 0.7$, and 1.2 , respectively. The dotted and long-dashed curves give Y for $\alpha = 0.3$, and $u = 0.6$ and 0.1 , respectively. The short-dashed curve gives Y^0 , the yield in the pair rest mass alone for $\alpha = 0.7$. The dot-dashed curve gives the maximum possible Y at a given Θ , which corresponds to Comptonized bremsstrahlung with no ambient soft photons at $\tau_p = 0$ (it is almost the same as the solid curve in panel a). A slightly lower Y with a maximum of 0.25 at $\Theta \simeq 0.4$ is obtained in the case of soft-photon Comptonization for $\alpha = 0.14$. (d) $Y(\ell_{\text{tot}})$. The meaning of curves is the same as in (c).

α and Θ (rather than τ and Θ) as independent parameters. Furthermore, we take u (rather than τ_p) as an independent parameter. Also, we consider pair escape in some models, which adds one more independent parameter, β . Thus, a model is specified by α , Θ , u , and β (as in Z85). (In addition, there is some secondary dependence on n_p for the bremsstrahlung emission only, see Section 2.1.) The pair equilibrium condition [pair production rate = pair annihilation rate + pair escape rate, see equation (20) in Z85] uniquely determines the ratios of the Wien and power-law photon densities to the electron density, respectively N_W/n_e and N_P/n_e . Note that our formalism implicitly assumes that there is an appropriate supply of seed soft photons to ensure photon balance. The solution of the pair equilibrium equation gives the compactness parameters corresponding to the two components of the radiation field (power-law and Wien) described by equation (16),

$$\ell_W = 4\pi \frac{N_W}{n_e} \frac{\Theta \tau}{1 + \tau_W(\Theta)/3} \quad (17)$$

[where the radiative transfer is treated as in equation (9)], and

$$\ell_P = \frac{2\pi}{3} \frac{N_P}{n_e} \Theta E(\alpha) \min(1, \tau), \quad (18)$$

where

$$E(\alpha) \equiv \int_{\epsilon_s/\Theta}^{\infty} t^{-\alpha} e^{-t} dt \quad [\simeq \Gamma(1-\alpha) \text{ for } \alpha < 1], \quad (19)$$

and $\epsilon_s = 0.002$ is assumed. The total power escaping the source, which in steady state equals the total power supplied to the source, has a corresponding compactness parameter,

$$\ell_{\text{tot}} = \ell_W + \ell_P + \ell_{\text{ann}} + \ell_{\text{esc}} + \ell_{\text{brem}} \quad (20)$$

[where ℓ_{brem} is given by equation (14)].

As bremsstrahlung always operates in a plasma, we examine here its importance for the models considered here. A pair-equilibrium plasma *without* ambient photons is characterized by a pair of values, Θ , τ , as discussed in Section 2.1. This pair implies in turn some value of $\alpha(\Theta, \tau)$, the spectral index of the power-law component of the spectrum from Comptonization of ambient photons, as discussed above. However, since that plasma is already in pair equilibrium, addition of ambient soft photons at any non-zero amplitude and their subsequent Comptonization result in extra pair production, which would then violate pair equilibrium. Thus, this α represents a critical spectral index, $\alpha_{\text{cr}}(\Theta, u)$, which bounds from below the allowed

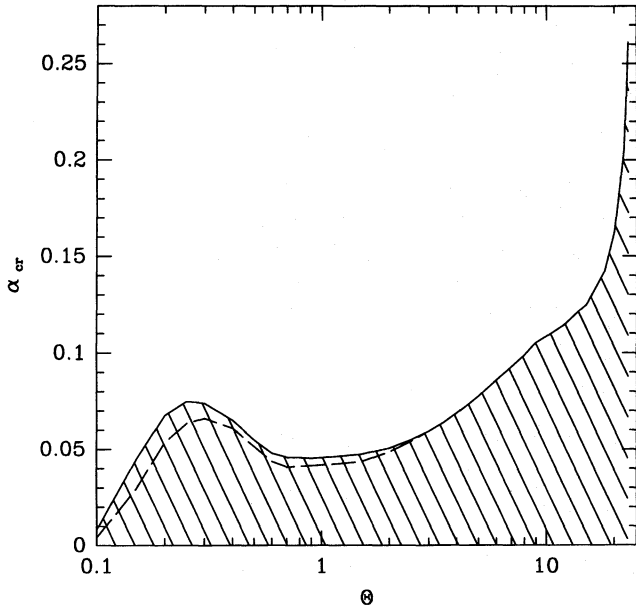


Figure 2. The minimum $\alpha = \alpha_{\text{cr}}$ for which pair equilibrium can be maintained. It corresponds to τ and Θ at which Comptonized bremsstrahlung alone results in pair equilibrium in pure pair plasmas ($u = 1$). The density is $n_e = 10^{10} \text{ cm}^{-3}$ (typical for AGNs) for the solid curve and 10^{16} cm^{-3} (typical for Galactic compact objects) for the dashed curve. The hatched region shows the range of α – Θ where no pair equilibrium is possible.

range of spectral indices of Comptonization of ambient soft photons.

Fig. 2 shows $\alpha_{\text{cr}}(\Theta, u = 1)$, i.e., for pure pair plasmas. Since α_{cr} increases with decreasing u , the values shown give the overall minima of α_{cr} at any u . We see that α_{cr} depends weakly on Θ and has typical values $\alpha_{\text{cr}} \sim 0.1$ – 0.2 . There is also a weak dependence on n_e , via the bremsstrahlung self-absorption energy, ϵ_m . Specifically, an increase of n_e for $\Theta \lesssim 1$ enlarges slightly the region in which pair equilibrium can be achieved. The solid and dashed curves in Fig. 2 correspond to n_e expected in AGNs and Galactic compact sources, respectively (taking $\tau \sim 1$ and typical sizes of those sources). The hatched region shows the parameters for which the plasma is out of pair balance. Plasmas with parameters above the curves can be in pair equilibrium for an appropriate amplitude of ambient soft photons. Comptonized bremsstrahlung dominates in the vicinity of α_{cr} , but its importance decreases rapidly with increasing α . We found numerically that bremsstrahlung can be neglected for $\alpha \gtrsim \alpha_{\text{cr}} + 0.05$.

Figs 1(c)–(d) show the values of Y in models without pair escape. The pair yield decreases with increasing α , and, for $\alpha > 0.41$, $Y \lesssim 0.1$ at any Θ . The pair yield is maximized at $\alpha = \alpha_{\text{cr}}$, where it equals that for pure Comptonized bremsstrahlung. However, no Comptonization of ambient soft photons is then allowed, as discussed above. We have found that the maximum Y in plasmas with dominant soft photon Comptonization occurs for $\alpha = 0.14$ and $\Theta = 0.4$, when $Y = 0.25$ and $Y^0 = 0.15$, which are just slightly below the corresponding maxima for pure Comptonized bremsstrahlung. This maximum occurs at $\ell_{\text{tot}} \simeq 20$ (Fig. 1d).

For a given α , Y decreases rapidly below $\Theta \sim 0.2$ due to most photons being below the threshold for pair production.

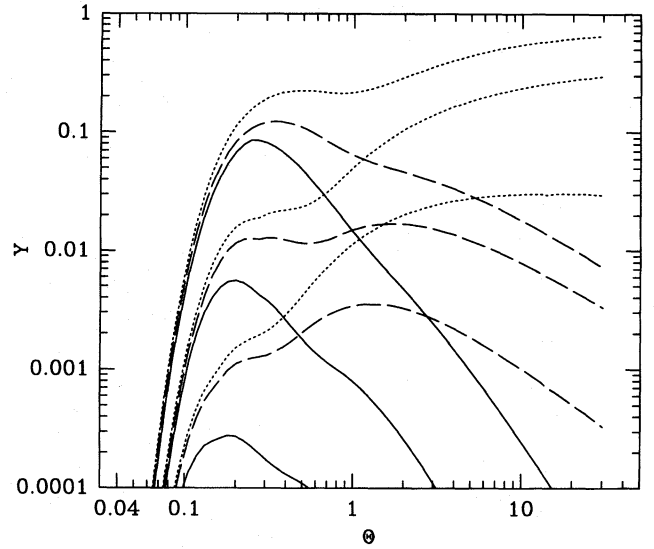


Figure 3. The pair yield in plasmas with Comptonization of ambient photons and pair escape at $\beta = 0.6$. The dotted, dashed and solid curves show Y_{esc} , Y_{esc}^0 and Y_{ann} , respectively, for $\alpha = 0.3, 0.7$, and 1.2 (from top to bottom).

The decrease of Y above $\Theta \sim 0.3$ – 1 (depending on α) results from the decrease of both the annihilation cross-section and the optical depth, which cause a decrease of the pair annihilation rate. For $\Theta \gtrsim 20$, the pair production rate due to electron–electron interactions (which is independent of the photon density) becomes comparable to the pair annihilation rate. The pair equilibrium can be maintained only for small photon densities, which implies small ℓ_p and ℓ_w . For $\alpha \gtrsim 0.3$, this results in Y increasing again above $\Theta \sim 20$. However, Y^0 is then negligibly small (see the short-dashed curve in Fig. 1b), which makes this increase unimportant. For $\alpha \lesssim 0.3$, bremsstrahlung dominates at $\Theta \sim 20$ (see Fig. 2) and Y does not increase as the annihilation to bremsstrahlung emissivity ratio decreases with the increasing Θ (see Appendix). At $\Theta > 24$, there are no more equilibrium solutions as the pair annihilation cannot keep up with the pair production (Svensson 1982; Zdziarski 1982).

The pair yield is maximized in pure pair plasmas ($u = 1$). A decrease of u (corresponding to an increase of τ_p) results in a decrease of Y (see Fig. 1b).

Fig. 3 shows Y_{ann} , Y_{esc} and Y_{esc}^0 in models with pair escape [we assume here $\beta = 0.6$ corresponding approximately to the escape velocity of pairs equal to the maximum value of the sound speed in a relativistic gas (Synge 1957)]. Y_{ann} is less than one-half of that in models without pair escape with the same Θ and α . Y_{esc}^0 is the largest for $\Theta = 0.2$ – 1.2 . At higher temperatures, Y_{esc}^0 decreases due to the increase of the average photon energy (which gives fewer pairs per unit photon energy). For models with $\alpha > 0.38$, Y_{esc}^0 does not exceed 0.1 at any temperature. For $\alpha = 0.1$, Y_{esc}^0 has the maximum value of $Y_{\text{esc}}^0 = 0.16$ at $\Theta = 0.34$. For $\Theta > 0.3$, most of the power converted into pair energy has the form of kinetic energy of escaping pairs, with Y_{esc} increasing with increasing temperature. For $\alpha = 0.3$, Y_{esc} exceeds 0.1 for $\Theta > 0.18$ and rises to ~ 0.65 at $\Theta \gg 1$. The value of ~ 0.65 is the highest value of Y_{esc} (for $\beta = 0.6$) as a decrease of α below ~ 0.3 implies a decrease of the pair escape rate (due to the corresponding

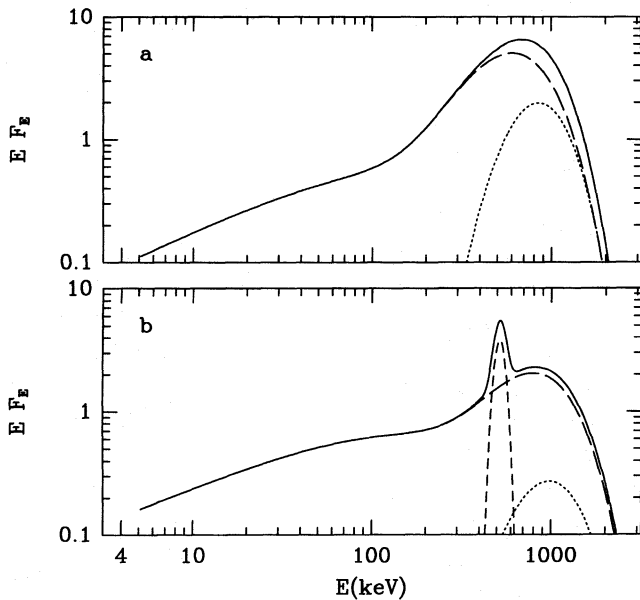


Figure 4. Spectra from thermal pair-equilibrium plasmas. The dashed, dotted, and solid curves give the Comptonization spectrum [equation (16)], the spectrum from annihilation inside the source, and the total emitted spectrum, respectively. (a) No pair escape, $\alpha = 0.3$, $\Theta = 0.3$, and $u = 1$, which gives $Y = 0.18$. Even at this large Y , the annihilation feature is not visible. (b) Pair escape at $\beta = 0.6$ and cooling outside the source for $\alpha = 0.4$ and $\Theta = 0.4$. The short-dashed curve gives the spectrum of annihilation outside the source at the assumed temperature of 5 keV. The narrow feature contains 12 per cent of the plasma luminosity.

increase of τ , which becomes ~ 1 in that regime). However, this Y_{esc} corresponds to negligible Y_{esc}^0 , as shown in Fig. 3, as well as to the corresponding annihilation emission at $\Theta \gg 1$ being dominated by bremsstrahlung emission (see Appendix). Thus, this maximum has no observable consequences and we will not consider it further.

A very interesting observational question is that of the possibility of observing an annihilation line from thermal plasmas. Fig. 4 shows example spectra of plasmas in which copious pair production ($Y > 0.1$) occurs. We use formulae from Svensson (1983) for the spectrum of optically thin thermal annihilation.

Although a large fraction of the power delivered to the source may be converted into the energy of pairs that annihilate in the source, in no case does annihilation result in a distinct, observable line-like feature. As discussed earlier, large Y requires $\Theta > 0.1$. In that case, however, the annihilation spectrum is broad and difficult to distinguish from the Wien bump (which is formed at energies $\sim 3kT$). Thus the annihilation feature only slightly modifies the primary spectrum (see Fig. 4a). Furthermore, at $\Theta \gtrsim 3$, the $e^\pm e^\pm$ bremsstrahlung spectrum alone dominates the annihilation spectrum (see Appendix).

In models with strong pair escape, most of the pair energy is carried away by the outflowing pairs. If the temperature of pairs remains constant during their escape, then for $\alpha < 0.7$ and $\Theta \simeq 0.3$ –1 the broad annihilation spectrum produced by the annihilation of the escaping pairs can contain more than 10 per cent of the source luminosity. However, the modification of this spectrum by the addition of the Wien photons from the

source again gives a feature with a width and shape different from those expected for annihilation. At $\Theta \gtrsim 1$, annihilation both inside and outside (where no pair cooling is assumed) the source results in a broad hump formed at $\sim m_e c^2 + (2-3)kT$. At $\Theta \gtrsim 3$, the annihilation spectrum becomes negligible in comparison with that from $e^\pm e^\pm$ bremsstrahlung (see Appendix). Also, for $\Theta \gg 1$ and $\tau \ll 1$, the profiles from individual Compton scatterings may be distinctly seen in the total spectrum, in which case they can no longer be approximated by a power law (Haardt 1993).

On the other hand, escaping pairs may lose their energy via adiabatic or Compton cooling. If they cool down to energies $\lesssim 10$ keV, the total spectrum will show a distinct narrow line, as shown in Fig. 4(b). The ratio of the luminosity contained in the narrow line to the total source luminosity is given by Y_{esc}^0 .

3 NONTHERMAL PLASMAS

In nonthermal plasmas, relativistic electrons or pairs are injected (e.g., monoenergetically or with a power-law distribution) with power corresponding to the compactness, ℓ_e . Nonthermal electrons produce γ -rays through Compton up-scattering of soft photons from a photon source that has an analogous compactness ℓ_s . The γ -rays are absorbed in photon-photon collisions giving rise to an e^\pm cascade. As a result of rapid Compton cooling, the pairs reach sub-relativistic energies before thermalizing and annihilating (see e.g., Svensson 1987; Lightman & Zdziarski 1987).

The pair yield Y^0 in nonthermal plasmas has been studied by, e.g., Svensson (1987), Lightman & Zdziarski (1987), and Done et al. (1990). For electron injection at Lorentz factors so large that the first-order Compton scattering spectrum extends above the threshold energy for pair production, 511 keV, the pair yield is mostly a function of ℓ_e . (For conditions typical of those in AGN, this would require injection Lorentz factors $\gamma_i \gtrsim 100$.) The dependence can then be very roughly approximated as $Y^0 \simeq 0.1(\ell_e/50)$ for $\ell_e < 50$ and saturating at $Y^0 \sim 0.1$ for $\ell_e > 50$ (Lightman & Zdziarski 1987).

When most of the electrons are injected at lower Lorentz factors than this, Y^0 strongly depends on the typical electron injection energy. The case of monoenergetic injection at Lorentz factor γ_i is discussed in Done et al. (1990, see fig. 1 there). At $\gamma_i \lesssim 3$, there is no or very little pair production in any models. At higher Lorentz factors, there is a fast increase of Y^0 with γ_i , up to 0.1 at $\gamma \gtrsim 10^2$. There is an intermediate plateau of Y^0 corresponding to Lorentz factors such that the second-order scattering spectrum extends above 511 keV. There is also a dependence on the ratio of the compactness in the electrons and the soft photons, ℓ_e/ℓ_s .

The same qualitative behaviour also applies when the electrons are injected with a spread of energies. Fig. 5(a) shows a sample calculation (using the model of Coppi 1992) of Y^0 when electrons are injected with a power-law energy distribution ($N(\gamma) \propto \gamma^{-\Gamma}$) and the injection index is varied. For $\Gamma \sim 1$, most of the injected luminosity is carried by electrons with $\gamma \sim \gamma_{\text{max}}$. The first-order Compton spectrum then has a significant amount of power at photon energies above the pair production threshold, and Y^0 is correspondingly large. The pair yield and emergent spectrum obtained are in fact very close to those for the case of monoenergetic injection at

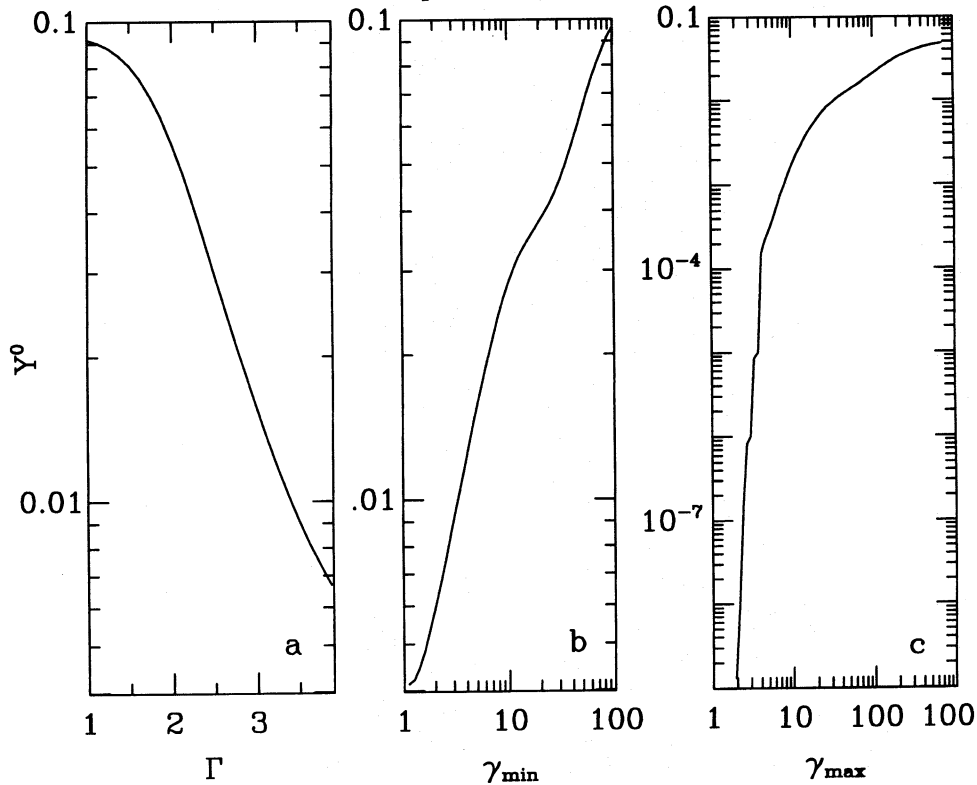


Figure 5. Pair yield, Y^0 , in a nonthermal plasma with power-law injection of primary electrons as a function of (a) the power-law injection index, Γ (the electrons are injected with Lorentz factors between $\gamma_{\min} = 5$ and $\gamma_{\max} = 10^3$), (b) the minimum electron injection energy, γ_{\min} (at fixed $\gamma_{\max} = 10^3$ and $\Gamma = 3$), and (c) the maximum electron injection energy, γ_{\max} (at fixed $\gamma_{\min} = 1.2$ and $\Gamma = 2$). The model compactnesses are $\ell_e = 80$ and $\ell_s = 30$, and the temperature of the ambient soft (blackbody) photons is $kT_{\text{BB}} = 10$ eV.

$\gamma_i = \gamma_{\max}$. As Γ is increased, more and more of the injected luminosity is carried by low-energy electrons with $\gamma \sim \gamma_{\min}$ and the amount of power in the first-order Compton spectrum that is above the pair production threshold drops. Since less energy is available to produce pairs, the pair yield drops as $\Gamma \rightarrow \infty$, rapidly approaching the value obtained for monoenergetic injection at $\gamma_i = \gamma_{\min}$. Fig. 5(b) shows a similar case where the injection spectrum is a steep power law ($\Gamma = 3$) and most of the injected luminosity is carried by electrons injected at $\gamma \sim \gamma_{\min}$. As γ_{\min} is decreased in this example, the number of upscattered photons with energies exceeding the pair production threshold again decreases, and Y^0 drops rapidly. If one holds γ_{\min} fixed and instead decreases γ_{\max} , the effect on Y^0 is the same (Fig. 5c).

In general, when the compactness ℓ_e is high and most electrons are injected at high energies, the pair yield in a nonthermal plasma can be significant. However, the yield is limited to $Y^0 \lesssim 0.1$ unless $\ell_s \ll \ell_e$, i.e., the plasma is photon-starved. For photon-starved nonthermal plasmas, the maximum pair yield among models considered by Zdziarski et al. (1990) is larger, $Y_{\max}^0 \approx 0.25$, similar to the case of thermal plasmas with hard spectra (Section 2), which are in fact also soft photon-starved.

Since the pairs produced typically have time to cool to sub-relativistic energies before annihilating, the annihilation spectra produced are usually narrow and not easily hidden by continuum photons. Thus, in contrast to the case of a thermal plasma, nonthermal plasmas tend to have observable annihilation features as long as the pair yield is large enough (see, e.g., the figures in Lightman & Zdziarski 1987). The one

notable exception to this is the case where most electrons are injected at low energies as in the examples of steep power-law injection considered above. To obtain a high pair yield, the plasma must be very compact and photon-starved. The annihilation features produced in this case are broad and often difficult to distinguish from the Wien-like features produced by Compton scattering (see Zdziarski et al. 1990). Generally, the spectra produced when primary electrons are injected at very low energies strongly resemble those produced by thermal plasmas (Ghisellini, Haardt & Fabian 1993) and do not show strong annihilation features as the pair yield is small. If Seyfert AGN spectra are thermal in origin or are produced by nonthermal plasmas with low-energy electron injection, we therefore do not expect higher sensitivity observations to find strong annihilation features in their spectra.

4 APPLICATIONS TO COSMIC GAMMA-RAY SOURCES

4.1 The annihilation feature in Nova Muscae

In Section 2.2, we found that if thermal pairs escape the source and cool down to low energies before annihilating then a narrow line may be seen in the spectrum of the source. A narrow line at ~ 480 keV, which is possibly a redshifted annihilation line, was observed in the spectrum of Nova Muscae (Sunyaev et al. 1992). We point out, however, that the spectrum of Nova Muscae shows a power-law-like continuum between 20 keV and 70 keV with $\alpha \sim 0.9$ which softens above 70 keV to

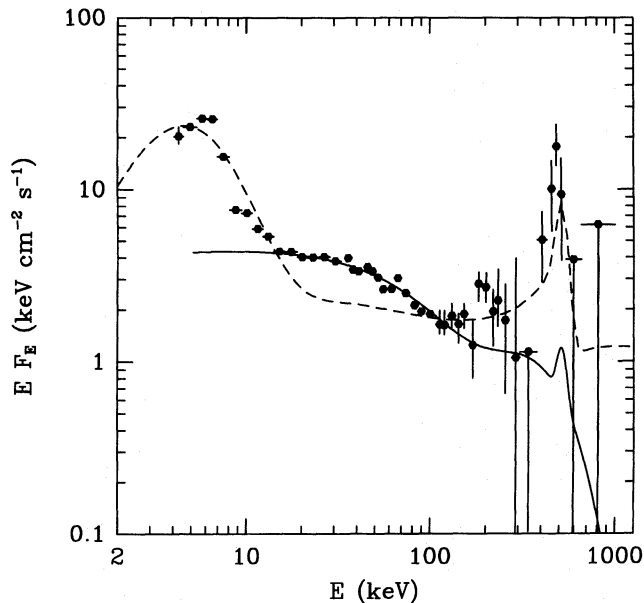


Figure 6. The spectrum of Nova Muscae with a line at ~ 480 keV observed on 1991 January 21 (Sunyaev et al. 1992). The solid curve shows the spectrum of a thermal model with $\alpha = 0.9$ and $\Theta = 0.16$ with pairs escaping with $\beta = 1$ and cooling down to 3 keV. These parameters yield $Y = 7.3 \times 10^{-3}$, which is much too small to explain the observed line. The dashed curve gives our best nonthermal model of the spectrum. The compactnesses are $\ell_e = 60$ and $\ell_s = 120$, $kT_{\text{BB}} = 1$ keV, and nonthermal electrons are injected monoenergetically with the Lorentz factor $\gamma_i = 10^3$. The pair yield is again insufficient to explain the strong line. Both thermal and nonthermal pair production models are ruled out.

$\alpha \sim 1.4$. For such a spectrum, Y does not exceed 0.01 (even for $\beta \sim 1$) whereas the observed feature contains as much as 30 per cent of the luminosity above 20 keV (see Fig. 6).

We have also attempted to explain the spectrum of Nova Muscae by nonthermal pair models (as described in Lightman & Zdziarski 1987). First, we have found no nonthermal model that could fit the continuum spectrum entirely. Secondly, any nonthermal model with the spectrum lying below the observed one (i.e., allowing for another continuum spectral component) has a pair yield too small to explain the large strength of the annihilation feature. Our best model is shown in Fig. 6.

Thus, our findings rule out simple models of pair production (either thermal with pair escape or nonthermal) in that object. On the other hand, obscuration of the region producing the continuum spectrum (where the pairs are produced) can possibly explain the large relative strength of the annihilation feature. However, such obscuration models need to be complex since the strength of a feature at ~ 200 keV interpreted as a Compton-reflected annihilation line is so large that obscuration of the region where the pairs annihilate is required as well (Hua & Lingenfelter 1993).

4.2 e^\pm pairs in AGNs

The observation of NGC 4151 by OSSE (Maisack et al. 1993) shows a break in the spectrum at energy ~ 100 keV and puts an upper limit on the e^\pm annihilation flux, which rules out fully nonthermal models (Zdziarski et al. 1993). The latter authors also show that the spectrum is relatively well-fitted

by a thermal model with $\alpha = 0.6$ (constrained by a *Ginga* observation, see Yaqoob et al. 1993) and $kT = 43$ keV. The solution of the pair equilibrium equation for these parameters at $u = 1$ gives a very high value of the compactness, $\ell = 9000$. Such a compactness cannot be achieved in an accreting source as it exceeds the Eddington value of $\sim 10^3(10R_G/R)$, where R_G is the Schwarzschild radius (Svensson 1987). Thus if the emitting plasma is purely thermal it must be e^- -dominated ($u \ll 1$). As even for a pure pair plasma with the above parameters the pair yield is $\lesssim 10^{-3}$, we do not expect to observe an annihilation feature.

On the other hand, the observation may be explained by a hybrid thermal–nonthermal model (Zdziarski et al. 1993) with $\lesssim 40$ per cent of the power released nonthermally and the remaining power dissipated thermally in the source. In that case, the presence of nonthermal particles results in efficient pair production, and a modest nonthermal compactness of $\ell_e \sim 30$ (required by the best fit of the model) is sufficient for the source to be e^\pm -dominated. An annihilation feature close to the level of the sensitivity of OSSE is predicted.

The OSSE observation of another AGN, IC 4329A, was discussed by Zdziarski et al. (1994), who concluded that the γ -ray emitting plasma can form a thermal corona above the surface of an accretion disc. The corona can be e^\pm -dominated for a compactness $\ell_e \simeq 10^2$, or e^- -dominated for much lower compactness. An additional effect possible in the corona geometry is diffusion of pairs from the corona to the disc. If that process proceeds efficiently, the thermal corona has to be e^- -dominated at any compactness below the Eddington limit, similarly to the case of NGC 4151. No pair annihilation feature is expected. This is also the case in nonthermal models with electron injection at a very low $\gamma_i \sim 3$ (Zdziarski et al. 1994).

On the other hand, pair escape has little effect on the pair-dominated nonthermal model for that source [with a power-law electron injection, Zdziarski et al. (1994)]. In the model, a distinct annihilation feature containing ~ 5 per cent of the X-ray/ γ -ray luminosity (within the OSSE upper limits) is predicted. The presence or absence of such a feature can be established in the future, which will serve as a sensitive test distinguishing between thermal and nonthermal models.

4.3 The annihilation feature of the 1979 March 5 gamma-ray burst

The spectrum of the initial pulse of the March 5 γ -ray burst shows a clear emission feature centred at 430 keV (Mazets et al. 1982), which has been interpreted as annihilation radiation redshifted in a gravitational field. The feature contains ~ 7 per cent of the total energy flux of the impulsive phase. We have found that the spectrum is consistent with that predicted by the thermal model with pairs escaping and cooling outside the source, as shown in Fig. 7. Following Mazets et al. (1982), we have fitted the soft component by an exponential spectrum. The possible identification of the burst with a supernova remnant in the LMC (Evans et al. 1980) implies a luminosity during the impulsive phase of $\sim 3 \times 10^{44}$ erg s^{-1} . The fitted thermal model gives a compactness of ~ 10 , which at the above luminosity implies a source size of $\sim 10^{15}$ cm. This contrasts with the rise time of the impulsive phase of < 0.2 ms, which implies an emission region of size $\sim 10^7$ cm in the absence of beaming. On the other hand, beaming

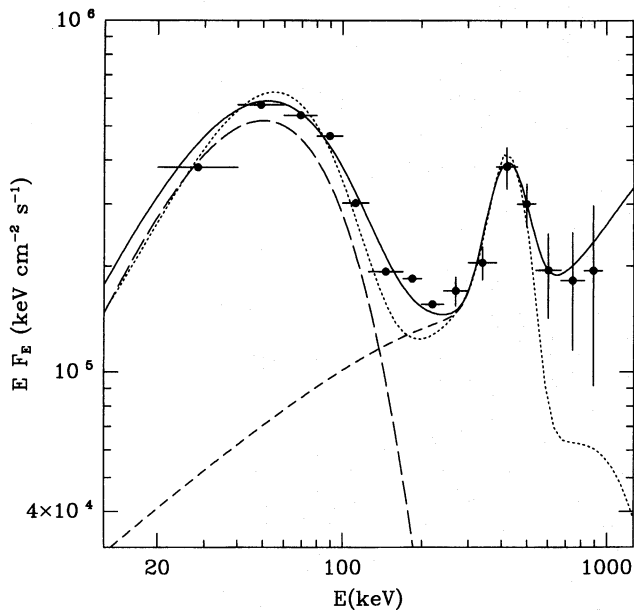


Figure 7. The spectrum (filled circles) of the initial pulse in the 1979 March 5 γ -ray burst as observed by *Venera 11* (Mazets et al. 1982). The short-dashed curve gives the spectrum from our thermal model with $\Theta = 1$, $\alpha = 0.34$ and $u = 1$ and with pairs escaping at $\beta = 0.6$ and cooling down to 25 keV. Only the annihilation line is redshifted by $z = 0.32$ (which would correspond to pairs created away from a neutron star but annihilating at its surface). The soft component is fitted by $F_E \sim \exp(-E/25 \text{ keV})$ (long-dashed curve). The resulting sum of the soft and hard spectra (solid curve) fits the observed spectrum well. The dotted curve shows the fit of a nonthermal model with $\ell_e = 180$, $\ell_s = 1.2$, $kT_s = 30 \text{ eV}$, $\gamma_i = 10^3$, and with acceleration of relativistic electrons at an efficiency of 0.78. The total nonthermal spectrum is redshifted by $z = 0.2$.

of the emission region (which increases the estimated size of the emission region) would result in a strong blueshift of the feature. Thus, the presence of an annihilation feature in the spectrum is not consistent with the burst localization in the LMC, and our fit implies a distance of $\lesssim 5 \text{ pc}$.

A compactness of ~ 200 is implied by our fit of a non-thermal pair model with part of the power released thermally, as in Zdziarski et al. (1993), shown by the dotted curve in Fig. 7. Assuming a source size $\lesssim 10^7 \text{ cm}$, this compactness corresponds to a distance of $\lesssim 25 \text{ pc}$.

5 CONCLUSIONS

We find that no visible annihilation feature can be produced in thermal sources in pair equilibrium. This confirms previous Monte Carlo results of Zdziarski (1984, 1986). The invisibility of annihilation features is due to a combination of the effects of the formation of a Wien spectrum at low pair temperatures and high optical depth and of thermal broadening of the annihilation spectrum at high pair temperatures.

Although pair annihilation features from thermal plasmas are not distinguishable from the continuum, large numbers of pairs may still be produced in such plasmas. The main requirement for the pair yield to be large ($Y \gtrsim 0.1$) is that the continuum spectrum be hard, $\alpha \lesssim 0.4$. This is the case when plasma bremsstrahlung emission is the only source of

soft photons or when the plasma optical depth and temperature are sufficiently high. Maximum values of $Y \simeq 0.3$ and $Y^0 \simeq 0.2$ are obtained for Comptonized bremsstrahlung and soft-photon Comptonization with $\alpha \sim 0.1\text{--}0.2$ (as well as for photon-starved nonthermal plasmas, Section 3). The maxima occur at the total compactness of about 20. If there is also efficient pair escape from thermal sources, the pairs can annihilate outside the sources after adiabatic and radiative cooling. Narrow, distinct annihilation lines may be visible in this case.

We have also found that the spectral index of the power-law component in the spectrum of Comptonization of ambient soft photons is constrained by the pair-equilibrium condition to be $\alpha \gtrsim 0.1\text{--}0.2$, with a weak dependence on temperature. These minima correspond to $\alpha(\Theta, \tau)$ achieved in pair-equilibrium plasmas with Comptonized bremsstrahlung emission alone.

We have obtained the pair yield in nonthermal models with a power-law electron injection. The pair yield increases with increasing γ_{\min} , γ_{\max} , and with decreasing Γ . Narrow annihilation lines are predicted in most of the parameter space.

However, our calculations applied to the narrow annihilation line observed from Nova Muscae (Sunyaev et al. 1992) show that the continuum in that object is too soft to give rise to the required pair yield and models with either thermal or nonthermal pair production are not applicable to that object. Furthermore models of either thermal or nonthermal plasmas in pair equilibrium are unable to explain strong broad annihilation lines such as observed in 1E1740.7-2942 (Gilfanov et al. 1994) and the *HEAO 1* A-4 annihilation source (Briggs et al. 1995), as found by Maciołek-Niedźwiecki & Zdziarski (1994). Obscuration of the source of pairs appears to be necessary to explain those observations.

The γ -ray emitting plasma in NGC 4151 cannot be pair-dominated unless part of the power is released nonthermally in the source. On the other hand, the X-ray/ γ -ray source in IC 4329A can be thermal and pair-dominated if pair escape from the source is efficiently suppressed. That source is also compatible with nonthermal, pair-dominated models with a power-law electron injection (Zdziarski et al. 1994).

The annihilation feature observed in the 1979 March 5 γ -ray burst can be explained in terms of either a nonthermal model or a thermal one with pairs escaping and cooling outside the source. However, the implied maximum distance to the source is much less than that to the LMC, in which direction the burst occurred.

ACKNOWLEDGMENTS

We thank Roland Svensson for valuable comments on this work. This research has been supported in part by the NASA grants NAG5-2439, NAGW-3129, and NAG5-1813, and the Polish KBN grant 2P03D01008.

REFERENCES

- Björnsson G., Svensson R., 1991, *MNRAS*, 249, 177
- Briggs M. S., Gruber D. E., Matteson J. L., Peterson L. E., 1995, *ApJ*, 442, 638
- Coppi P. S., 1992, *MNRAS*, 258, 657
- Done C., Ghisellini G., Fabian A. C., 1990, *MNRAS*, 245, 1
- Evans W. D. et al., 1980, *ApJ*, 237, L7

- Ghisellini G., Celotti A., George I. M., Fabian A. C., 1992, MNRAS, 258, 776
 Ghisellini G., Haardt F., Fabian A. C., 1993, MNRAS, 263, L9
 Gilfanov M. et al., 1994, ApJS, 92, 411
 Haardt F., 1993, ApJ, 413, 680
 Hua X.-M., Lingenfelter R. E., 1993, ApJ, 416, L17
 Kusunose M., Zdziarski A. A., 1994, ApJ, 422, 737
 Lightman A. P., Zdziarski A. A., 1987, ApJ, 319, 643
 Maciołek-Niedźwiecki A., Zdziarski A. A., 1994, ApJ, 436, 762
 Madejski G. M. et al., 1995, ApJ, 438, 672
 Maisack M. et al., 1993, ApJ, 407, L61
 Mazets E. P., Golenetskii S. V., Guryan Yu. A., Ilyinskii V. N., 1982, Ap&SS, 84, 173
 Sunyaev R. et al., 1992, ApJ, 389, L75
 Svensson R., 1982, ApJ, 228, 335
 Svensson R., 1983, ApJ, 270, 300
 Svensson R., 1984, MNRAS, 209, 175 (S84)
 Svensson R., 1987, MNRAS, 227, 403
 Synge J. L., 1957, Relativistic Gas. North Holland, Amsterdam
 Yaqoob T., Warwick R. S., Makino F., Otani C., Sokoloski J. L., Bond I. A., Yamauchi M., 1993, MNRAS, 262, 435
 Zdziarski A. A., 1982, A&A, 110, L7
 Zdziarski A. A., 1984, ApJ, 283, 842
 Zdziarski A. A., 1985, ApJ, 289, 514 (Z85)
 Zdziarski A. A., 1986, ApJ, 303, 94
 Zdziarski A. A., Coppi P. S., Lamb D. Q., 1990, ApJ, 357, 149
 Zdziarski A. A., Lightman A. P., Maciołek-Niedźwiecki A., 1993, ApJ, 414, L93
 Zdziarski A. A., Fabian A. C., Nandra K., Celotti A., Rees M. J., Done C., Coppi P. S., Madejski G. M., 1994, MNRAS, 269, L55
 Zdziarski A. A., Johnson N. W., Done C., Smith D., McNaron-Brown K., 1995, ApJ, 438, L63

APPENDIX: $e^{\pm}e^{\pm}$ BREMSSTRAHLUNG AND ANNIHILATION

Pair annihilation radiation is always accompanied by $e^{\pm}e^{\pm}$ bremsstrahlung from the annihilating pairs. At mildly relativistic or lower temperatures, this bremsstrahlung emission can be neglected. However, the bremsstrahlung emissivity increases with Θ , whereas the annihilation emissivity decreases. As shown in fig. 1 of Svensson (1982), both emissivities are equal at $\Theta \simeq 3$. Consequently, annihilation radiation becomes negligible compared with bremsstrahlung at higher temperatures.

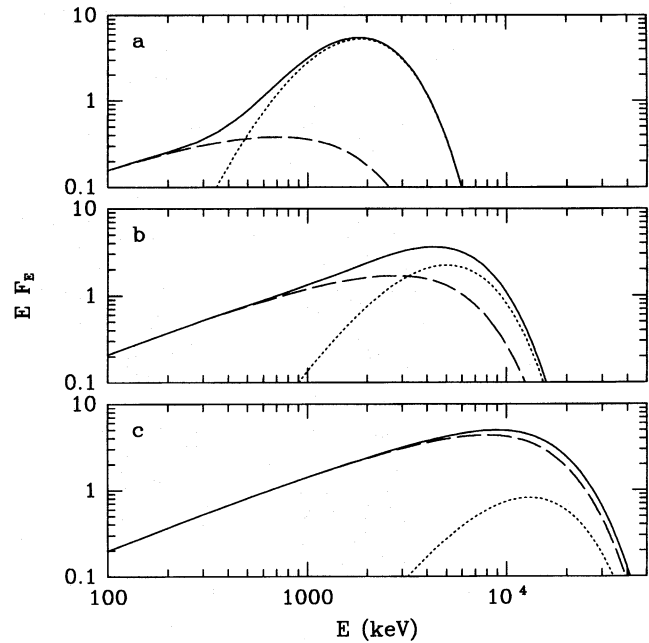


Figure A1. Spectral emissivities (equivalent to spectra in the limit of $\tau \rightarrow 0$) from relativistic e^{\pm} pair plasmas. The dashed curves show the $e^{\pm}e^{\pm}$ bremsstrahlung spectra, the dotted curves show the e^{\pm} pair annihilation spectra, and the solid curves show the sums of the two spectra. The plasma temperatures are (a) $\Theta = 1$; (b) $\Theta = 3$; (c) $\Theta = 8$.

Fig. A1 shows how the optically thin e^{\pm} annihilation and $e^{\pm}e^{\pm}$ bremsstrahlung spectra change with Θ in pure pair plasmas. One sees that the annihilation spectrum becomes negligible in comparison with the bremsstrahlung spectrum for $\Theta \gtrsim 3$. Both processes scale in the same way, i.e., their emissivities are proportional to the square of the plasma density, and it is not possible to avoid the $e^{\pm}e^{\pm}$ bremsstrahlung contribution to the spectrum. Thus, one cannot consider the pair annihilation alone (without the bremsstrahlung contribution) in a highly relativistic plasma.

This paper has been produced using the Royal Astronomical Society/Blackwell Science L^AT_EX style file.